TECHNICAL REPORT

ISO/TR 21900

First edition
2018-09

Guidance for uncertainty analysis regarding the application of ISO/TS 10974

Lignes directrices pour l'analyse de l'incertitude concernant l'application de l'ISO/TS 10974

Reference number
ISO/TR 21900:2018(E)

ISO copyright office
CP 401 • Ch. de Blandonnet 8
CH-1214 Vernier, Geneva
Phone: +41 22 749 01 11
Fax: +41 22 749 09 47
Email: copyright@iso.org
Website: www.iso.org

Published in Switzerland

Contents

Page

Foreword

ISO (the International Organization for Standardization) is a worldwide federation of national standards bodies (ISO member bodies). The work of preparing International Standards is normally carried out through ISO technical committees. Each member body interested in a subject for which a technical committee has been established has the right to be represented on that committee. International organizations, governmental and non-governmental, in liaison with ISO, also take part in the work. ISO collaborates closely with the International Electrotechnical Commission (IEC) on all matters of electrotechnical standardization.

The procedures used to develop this document and those intended for its further maintenance are described in the ISO/IEC Directives, Part 1. In particular, the different approval criteria needed for the different types of ISO documents should be noted. This document was drafted in accordance with the editorial rules of the ISO/IEC Directives, Part 2 (see www.iso.org/directives).

Attention is drawn to the possibility that some of the elements of this document may be the subject of patent rights. ISO shall not be held responsible for identifying any or all such patent rights. Details of any patent rights identified during the development of the document will be in the Introduction and/or on the ISO list of patent declarations received (see www.iso.org/patents).

Any trade name used in this document is information given for the convenience of users and does not constitute an endorsement.

For an explanation of the voluntary nature of standards, the meaning of ISO specific terms and expressions related to conformity assessment, as well as information about ISO's adherence to the World Trade Organization (WTO) principles in the Technical Barriers to Trade (TBT) see www.iso.org/iso/foreword.html.

This document was prepared by Technical Committee ISO/TC 150, *Implants for surgery*, Subcommittee SC 6, *Active implants*.

Any feedback or questions on this document should be directed to the user's national standards body. A complete listing of these bodies can be found at www.iso.org/members.html.

Introduction

Clause 8 of ISO/TS 10974:2018 describes methods (Tiers) for analyzing the RF power deposition for active implantable medical device (AIMD). EM evaluations in a complex near-field exposure scenario can be difficult and involve many uncertainty sources. Simulations requiring a model of the DUT and clinical incident field have uncertainties that need to be carefully assessed.

The objective of the uncertainty analysis is to determine the confidence interval of the RF-induced power deposition with respect to its true value. The acceptable level of uncertainty for an AIMD model is relative to the safety margin afforded by the AIMD's RF performance. For instance, if the expected MRI RF induced AIMD power deposition *in vivo* is very low, it is less critical to have a highly accurate model and more uncertainty can be tolerated in the model predictions.

Guidance for uncertainty analysis regarding the application of ISO/TS 10974

1 Scope

This document provides guidance for some methods that could be used to evaluate the sources of uncertainty. It is important to note that there are many legitimate methods for analyzing the overall uncertainty and that the methods in this document are illustrative only.

2 Normative references

The following documents are referred to in the text in such a way that some or all of their content constitutes requirements of this document. For dated references, only the edition cited applies. For undated references, the latest edition of the referenced document (including any amendments) applies.

ISO/TS 10974:2018, *Assessment of the safety of magnetic resonance imaging for patients with an active implantable medical device*

3 Terms and definitions

For the purposes of this document, the terms and definitions given in ISO/TS 10974 apply.

ISO and IEC maintain terminological databases for use in standardization at the following addresses:

— ISO Online browsing platform: available at https://www.iso.org/obp

— IEC Electropedia: available at http://www.electropedia.org/

4 Uncertainty background

4.1 General

The uncertainties are divided into random and systematic uncertainties.

Random errors result in measured values being distributed about the mean value. Measurement variations are often well approximated by normal or lognormal distributions. Many of the sources of uncertainty for the measurements described in this document are the result of exponential or r^n functions, e.g., the decay of power levels as a function of distance from the AIMD, and therefore can be approximated by lognormal distributions.

In addition to random errors, systematic errors should also be considered. Systematic error is the error remaining once the random error is removed as shown in Figure 1. Systematic errors should be eliminated wherever possible.

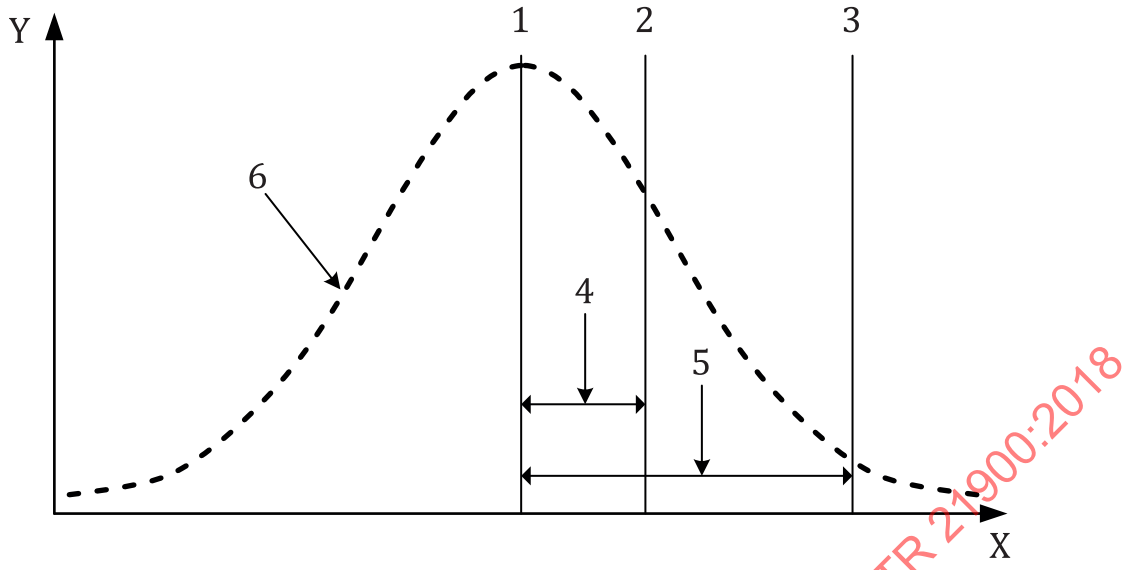

Key

X	range of values	Y	range of occurrence
1	mean value	4	random error
2	individual value	5	systematic error
3	true value	6	distribution of values

Figure 1 — Relationship of measured, mean, and true values and association of random and systematic errors

Uncertainty assessments of systems such as these can be dominated in magnitude by a small subset of uncertainty sources. When independent uncertainty sources are combined smaller uncertainty sources often contribute negligibly to the overall budget.

A variety of factors contribute to the uncertainty described in Clause 8 of ISO/TS 10974:2018. The dominant sources of uncertainty are specific to the equipment, measurement methods, and numerical simulation tools used for the assessment. Clause 8 of ISO/TS 10974:2018 requires an uncertainty assessment for the measurement system (u_{exp}) and AIMD model ($u_{Predict}$). There are two additional sources of uncertainty being clinical uncertainty (from 8.6 of ISO/TS 10974:2018) and power to temperature uncertainty (8.4.3 of ISO/TS 10974:2018). Techniques for evaluating these uncertainty terms (u_{exp}, $u_{Predict}$, $u_{Clinical}$, u_{Power}) are described. As Clause 8 of ISO/TS 10974:2018 has multiple tiers for evaluation of power deposition, the evaluation of each uncertainty source is specified per tier.

Two methods of uncertainty evaluations are developed in this document. In both methods, the uncertainty of the entire assembly is determined. In one method, many of the components of the assembly are grouped and a single uncertainty determination is made for many of them. In the second, the sources of uncertainty in a system are identified and individually evaluated a priori and the dominant sources are combined to obtain the system uncertainty.

GUM[1] has provided approaches for evaluating the uncertainty of assemblies, regardless of component count, and called their approaches Type A and Type B. Either or both Type A and Type B evaluations for each method is appropriate.

4.2 Method 1 Evaluation

Method 1 determines the uncertainty of a complex measurement system by considering the variability of the system as a whole. Method 1 is based on the assumption that a probability distribution of the random variation of the evaluation results can be deduced from approximation of the measurement or modelling system where the uncertainty is determined for an assembly or collection of many parts of the system. In this approach, multiple elements of the system are assembled or 'lumped' together and

their combined uncertainty is assessed. Estimates of the standard deviation of this distribution are obtained by repeated evaluations and statistical analysis of the obtained values.

4.3 Method 2 Evaluation

Method 2 generally dissects the assembly into its constituent parts, determines the uncertainty of each individually, and then determines the uncertainty of the group by combining the uncertainty of each of the components. Method 2 is based on reasonably assumed probability distributions that account for the available information about the quantities concerned, and the standard deviation of these distributions. This type of evaluation is performed by evaluating the independent sources of uncertainty of the components of the measurement or modelling system. In this approach, the components of the system are separated, and the uncertainty of each component is determined. In a subsequent step, the uncertainty of each is combined together. Techniques for handling the types of distribution of these uncertainties and normalizing to a standard distribution from non-standard distributions (such as rectangular, triangular, and U shaped) are well known[1]. Root sum square (RSS) is a common method for combining individual uncertainty components, however the method assumes that the terms are independent of each other.

In practice, some level of overlap between methods 1 and 2 is likely to exist in uncertainty evaluations.

5 Experiment Uncertainty (u_{exp})

5.1 General

The measurement system of Clause 8 of ISO/TS 10974:2018 is comprised of the RF field source, tissue simulating phantom, and probes for measuring temperature rise, SAR or E-field. It also comprises DUT fixturing to enable accurate positioning of the probe relative to the DUT. The parameter u_{exp} accounts for the combined uncertainty of the RF field source, tissue simulating phantom, the measurement probe, and the positioning of the measurement probe relative to the DUT.

5.2 Measurement tool uncertainty (probe)

For Clause 8 of ISO/TS 10974:2018, measurements of RF hotspots are done using SAR or temperature probes.

For SAR measurements, absolute measurements are necessary and the absolute accuracy is a contributor to the overall uncertainty. The absolute SAR uncertainty is determined from the calibration of the SAR probe. Depending on its use, the probes linearity, isotropy, distortion of the field, and noise level could influence its uncertainty.

For temperature probes, all temperature rise measurements are relative. Temperature probe placement accuracy will likely have a greater impact on measurement uncertainty than the repeatability of the temperature probe due to the spatial distribution of temperature.

5.3 Probe position uncertainty

Temperature or SAR decreases exponentially as a function of distance from the source of the RF hotspot. Therefore, probe positioning is an important contributor to the overall uncertainty.

Assuming a 10 °C peak temperature, a 1 °C temperature change can be observed in less than 250 µm. If ΔT measurements are accurate to within 0,1 °C, this is equivalent to better than 25 µm in probe placement accuracy. Therefore, temperature probe placement accuracy is one of the dominant sources of uncertainty and should be evaluated. When SAR probes are used, probe placement accuracy is equally important.

5.4 Tissue simulating phantom

In order to minimize differences between measurements and model predictions, it is desirable to control the conductivity of the TSM (tissue simulating medium) in addition to the background temperature. Background temperature control is necessary because conductivity and permittivity have large temperature coefficients as described in ISO/TS 10974:2018 Annex H.1.2. Permittivity is relatively insensitive to slight variation in mixing method and similar to conductivity, the variation during experiment can be controlled by limiting the bulk TSM temperature rise. TSM with various conductivity values within the tolerance range as specified in 8.3.2 of ISO/TS 10974:2018 can be used to evaluate the weighting coefficient for its contribution to the uncertainty in the temperature or SAR measurement.

5.5 RF field source

In order to minimize differences between measurements and model predictions, it is important to know the $E_{\tan}$ along the lead pathway matches the exposure assumed for prediction. It is typical to consider and control the RF incident fields along the lead pathway as well as the contribution of phantom position uncertainty to the RF Field uncertainty. Uncertainty of the RF incident fields along the lead pathway is more salient than field error at points in the phantom not near the lead pathways, and hence more useful to control and quantify.

Small changes in the lead pathway can produce a significant change in the measured ΔT, particularly for lead pathways that are producing significant phase cancelation or phase enhancement. The AIMD mounting fixture(s) and probe measurement fixture(s) need to be carefully designed in order to minimize the positional variation of the lead over the entire pathway. Small changes in the position of any section of the lead can change the magnitude or phase of the incident $E_{\tan}$ and result in a change in the measured ΔT or SAR.

The fixturing of the lead pathway on the RF field might distort an idealized simulation of this RF field and lead to uncertainty in the RF field source. Incident field distortion caused by fixturing could be a source of uncertainty, unless accounted for in the simulated incident fields from which $E_{\tan}$ along the lead pathways are derived.

5.6 Phantom position uncertainty

Uncertainty in the phantom position can also cause differences between the measured and simulated $E_{\tan}$ exposures leading to differences in the simulated and actual $E_{\tan}$ along the AIMD. This effect should be closely controlled or quantified as it can be a contributor to the overall uncertainty.

5.7 AIMD influence

The electric field induced in numerical human body models that do not contain AIMDs are used to define RF heating test environment specified in Tiers 2, and 3 of Clause 8. These methods assume that the perturbation of the induced electric field due to the AIMD can be neglected or is accounted for in the RF heating model validation. Care should be taken to ensure that these assumptions are valid for the AIMD being evaluated (particularly when multiple parts of the AIMD are in close proximity).

5.8 Overall $u_{\exp}$ consideration

The above description of a typical power deposition measurement system identified a number of contributors to the overall uncertainty.

In using a Method 2 analysis, the uncertainty of each of the above terms is determined. A specific experiment isolating each of these variables is evaluated, as much as reasonably possible. Then each of these individual contributions are combined using a RSS method to create an overall $u_{\exp}$.

In using a Method 1 analysis, an experiment or series of experiments are devised that combines the equipment or measurement components that are contributors to the overall uncertainty. The measurements from repeated experiments of these assemblies could use the probes (temperature

and/or incident E field), over the range of measurement probe placements, and over the range of TSM parameters, and the range of applied RF field are used to calculate a measurement variation, (i.e. temperature measurement variation/uncertainty).

6 AIMD model uncertainty (u_{Predict})

6.1 Piecewise excitation method for deriving AIMD model

Clause 8 of ISO/TS 10974:2018 does not describe a specific method for determination of the AIMD model, but contains Formula (1) for power deposition, P_{hotspot}, predicted by the AIMD model.

$$P_{\text{hotspot}} = A\left|\int_0^L S_{\text{hotspot}}(z)E_{\tan}(z)dz\right|^2 \tag{1}$$

where $E_{\tan}(z)$ is the incident tangential E field along the length of the lead. The AIMD model consists of A, the calibration factor and $S_{\text{hotspot}}(z)$, the transfer function along an AIMD of length L.

The piecewise excitation method[5] is one among several methods that can be used to derive $S_{\text{hotspot}}(z)$ for each AIMD hotspot. The piecewise excitation method involves measurement of the induced scattered complex E-field at the AIMD hotspot under test as the steady state response for each piecewise unit step $E_{\tan}$ applied at successive discrete locations along the length of the lead at the frequency of interest.

A typical piecewise excitation system consists of a source of localized $E_{\tan}$ that provides constant amplitude, constant phase piecewise excitation, an E-field sensor and test and measurement instrumentation such as RF source, oscilloscope, network analyzer, etc. The piecewise excitation system might be configured in a number of ways depending on the type of RF transmitter, sensor and test and measurement instrumentation. A schematic of one such configuration that uses a dipole transmitter, a coaxial monopole sensor and a vector network analyzer (VNA) is shown in Figure 2.

Methods used to measure and compute the calibration factor, A, that enables transformation of the relative total induced E-field amplitude from $S_{\text{hotspot}}(z)$ to an estimate of the power deposited for $E_{\tan}(z)$ are described in 8.4.3 and 8.4.4 of ISO/TS 10974:2018.

The $E_{\tan}(z)$ do not include any disturbance caused by the presence of the AIMD. This disturbance might depend on the proximity of one segment of the AIMD to the other and the construction of the AIMD. Caution should therefore be taken when using pathways with close AIMD segments such as the phase reversal (see ISO/TS 10974:2018, Annex M).

Either Method 1 or Method 2 may be used to determine uncertainty associated with the AIMD model, regardless of the technique for determining the AIMD model itself.

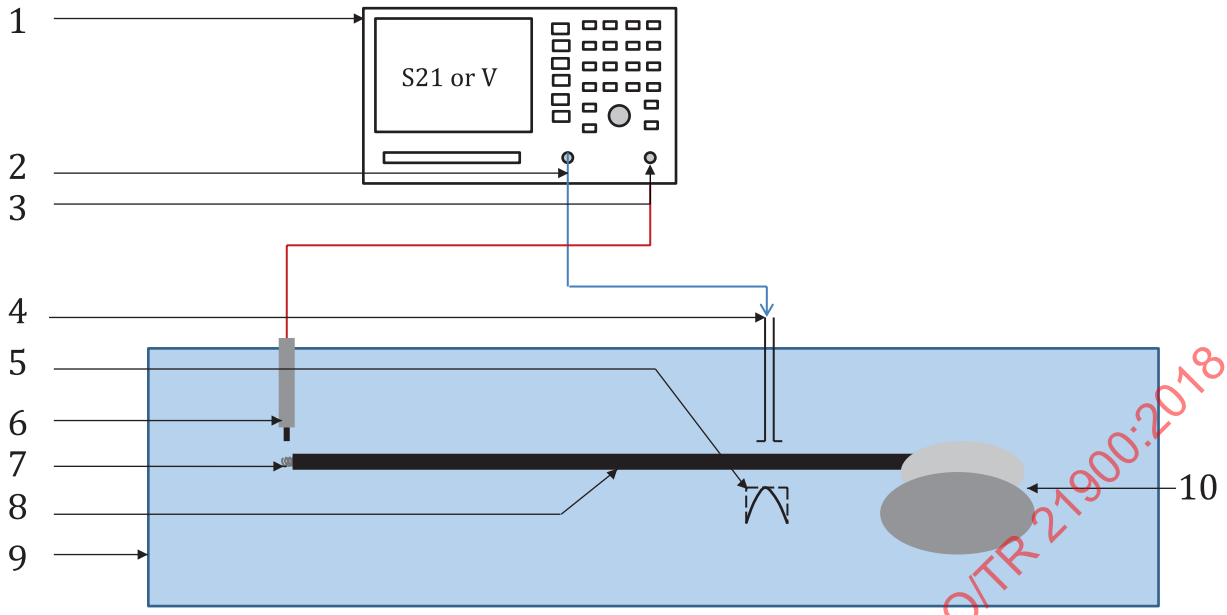

Key

1	RF source	6	coaxial antenna
2	port 1 of VNA	7	helical tip electrode
3	port 2 of VNA	8	length of the AIMD lead
4	dipole antenna	9	tissue simulating phantom
5	localized $E_{\tan}(z)$	10	AIMD device case

NOTE The test and measurement equipment (VNA) (1) consists of a RF source (2) (port 1 of VNA) and a sense input (3) (port 2 of VNA). The RF source is connected to a transmitting antenna [e.g., dipole antenna, (4)] that sets up a localized $E_{\tan}(z)$ (5) whose profile envelope can be approximated by a square. The scattered E field sense probe [e.g., coaxial antenna, (6)] is placed close to the AIMD hotspot of interest [e.g., helical tip electrode, (7)] so that the scattered E-field response to the piecewise incident $E_{\tan}$ is recorded as a S21 or voltage measure as a function of the location of the incident $E_{\tan}$ along the length of the AIMD (8). This is the transfer function, $S_{\text{hotspot}}(z)$. The AIMD, RF transmitting antenna and the sense probe are all located within a tissue simulating phantom (9).

Figure 2 — A typical measurement setup used to obtain $S_{\text{hotspot}}(z)$ with the piecewise excitation method

6.2 AIMD model uncertainty (u_{Predict}): Method 1

An equivalent electromagnetic model of the AIMD might have error in its predictions even when the incident tangential electric field along the AIMD is completely and accurately known. This subclause describes a method of determining the prediction error distribution and assigning a prediction uncertainty, u_{Predict}, to the AIMD model output assuming perfectly known incident field model input.

When using the AIMD model, its output is an estimate of the correct response to the input RF exposure along the AIMD, $E_{\tan}$ (l). The uncertainty of the output can be calculated based on differences between model predicted, P_{model}, and corresponding measured, P_{meas}, RF power deposition when the AIMD is exposed to a set of known radiated test conditions. The uncertainty depends on the RF power deposition measurement noise and on the choice of radiated test conditions among other factors.

The purpose of RF power deposition measurements is to estimate the correct response of the AIMD to a variety of known radiated test exposure conditions. Experimental controls should be incorporated to minimize measurement error as well as any differences between the assumed model input RF exposure along the AIMD and the actual applied radiated exposure during measurement. Errors in the RF field exposure, the surrounding tissue simulating media dielectric properties and the power deposition measurement (typically dominated by AIMD and measurement probe placement uncertainty) can

be quantified, minimized or otherwise controlled by making reference measurements of known or independent standards (e.g. performing a gauge repeatability and reproducibility study). Random measurement error contribution to the model prediction can be reduced by using an average or median value of multiple measured power deposition observations at each radiated test exposure. Radiated test exposure experimental designs which incorporate controls and replicate measurements as well as randomization of any remaining sources of error minimize the error contribution to u_{Predict}.

An example set of 25 AIMD radiated exposure predictions and corresponding power measurements are illustrated in Figure 3, with data values provided in Table 1. Each data point in the figure represents the mean value of replicate measurements, avg{P_{meas}}i, on the y-axis and the corresponding AIMD model prediction, P_{model},i, on the x-axis for each AIMD exposure $E_{\tan}$ (l)i tested. One method to quantify the uncertainty of the model prediction is to perform a linear regression between the measured dependent variable avg{P_{meas}} and the model predicted RF power independent variable P_{model} given by avg{ P_{meas}}i = β0 + β1 P_{model},i + ϵi where β0 and β1 are unknown constants that must be estimated and ϵi is a normally distributed random residual error for the AIMD exposure with zero mean and standard deviation of σ. For the case where no power is anticipated, the intercept β0 should be zero and the linear regression equation reduces to avg{P_{meas}}i = β1 P_{model},i+ϵi. In the case in which βo is not within the measurement uncertainty, the source of this systematic error should be examined. An example zero-intercept regression line is shown in Figure 3 with a β1 of 1,020 1 and statistical coefficient of determination (R^2) of 0,938 2. The β1 and R^2 values close to 1 demonstrate a deterministic and accurate regression relationship between model prediction and measurement.

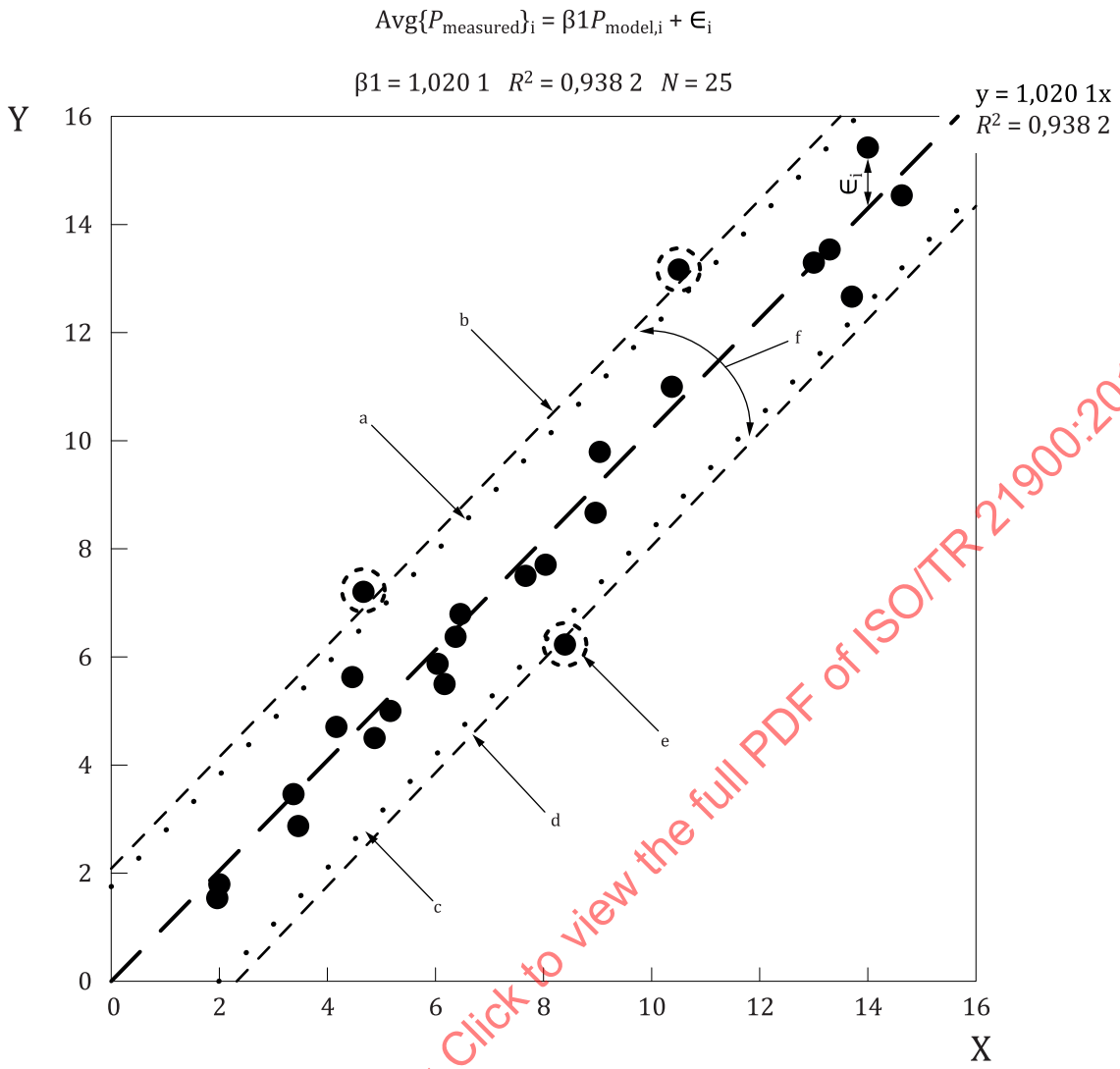

Key

X P_{model} for each ideal exposure

Y avg{$P_{measured}$} for each actual exposure

a Upper 90 % prediction interval bound.

b Upper 90 % tolerance interval bound.

c Lower 90 % prediction interval bound.

d Lower 90 % tolerance interval bound.

e Outlier.

f 95 % confident that there is 90 % chance the correct AIMD prediction lies between the Upper and Lower Tolerance Interval bounds.

Figure 3 — Linear regression for example set of 25 AIMD radiated exposure predictions and corresponding power measurements

Table 1 — Exposure values for Figure 3

P_{model} for each ideal exposure	Avg{$P_{measured}$} for each actual exposure
2,3	2,1
2,3	1,9
3,7	3,7
3,8	3,2
4,5	5
4,75	5,9
5	7,5
5,2	4,8
5,5	5,3
6,4	6,2
6,5	5,8
6,7	6,7
6,8	7,1
8	7,8
8,4	8
8,7	6,5
9,3	9
9,4	10,1
10,7	11,3
10,8	13,5
13,3	13,6
13,6	13,9
14	13
14,3	15,7
14,9	14,9

The residual errors ϵi provide an estimate of the uncertainty in the AIMD model prediction at each P_{model},i. The standard deviation σ of the model error distribution as a function of power deposition can be estimated from a trend line fit to the absolute value of the residual errors as shown in Figure 4[4]. The residual error is directly influenced by both the quality of the model and the quality of the RF power deposition experiments and should be minimized to reduce overall model output uncertainty. When measurement repeatability error is known, it can be removed from the model error by, for example, subtracting measurement error variance from the model error variance when defining the model error distribution or by averaging replicate measurements prior to regression analysis. The repeatability error is typically found by completing a gauge repeatability and reproducibility capability study of the measurement system.

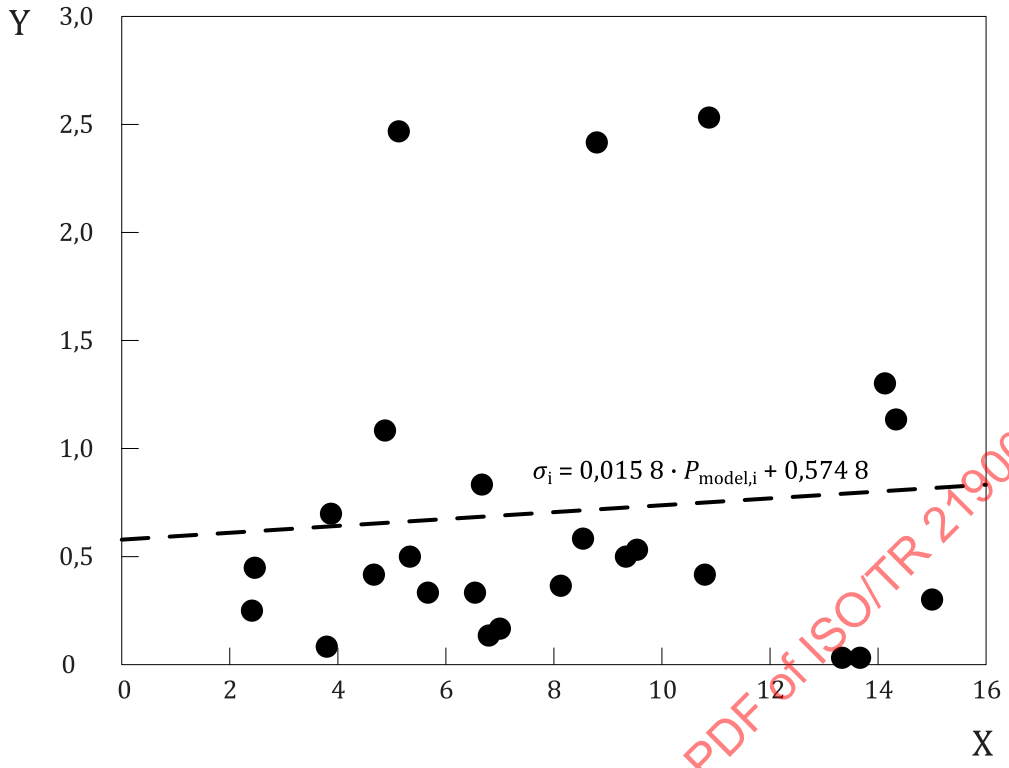

Key

X $P_{model,i}$ for each ideal exposure

Y residual error $\in_i$

Figure 4 — Absolute value of the residual errors for the example set of 25 AIMD radiated exposure predictions

The model uncertainty around a predicted value can be quantified from the regression analysis for a set of N radiated test conditions given a desired population coverage and desired confidence level by the Tolerance Interval (TI). The Confidence Interval for the mean response and Prediction Interval for a new observation are well-known[2]. To construct a Tolerance Interval, let $P_{meas,i} = \beta 1\ P_{model,i}$ be the regression predicted value for a given model input $P_{model,i}$. To calculate the Tolerance Interval at $P_{model,TI}$ for a desired population inclusion, D, a value of k must be found such that the probability of actual $P_{meas,i}$ being between ($\beta 1 P_{model,TI} - k^*\sigma$) and ($\beta 1 P_{model,TI} + k^*\sigma$) is D. The Wald-Wolfowitz approximation to k presented by Wallis[3] can be used in Formula (2), where:

$$k = r_{est}\sqrt{\frac{n}{\chi^2_{(1-C)}(n)}};\ r_{est} = K_p\left[1+\frac{1}{2N'}-\frac{2K_P{}^2-3}{24(N')^2}\right];\ N' = \frac{\sum_{i=1}^{N} P^2_{model,i}}{P^2_{model,TI}} \quad (2)$$

and the degrees of freedom n = N–1. For a desired confidence level, C, χ_(1–C)^2 (n) is the critical value from a chi-squared distribution with n degrees of freedom such that probability of the distribution being greater than χ_(1–C)^2 (n) is C. Kp is the critical value from a standard normal distribution with zero mean and variance of 1 such that the probability of the distribution absolute value being less than Kp is 1–D. For example, χ_(1 – 0,95)^2 (24) = 13,848 4 and Kp = 1,644 9 for N = 25, C = 95 % confidence and D = 90 % coverage of the example data in Figure 3.

Specifying the AIMD model uncertainty in this way allows matching the required level of accuracy in model prediction results to the associated AIMD RF hazard risk assessment with a known confidence level. The example regression plot in Figure 3 shows Tolerance Interval bounds indicating there is 95 % confidence that the true value lies within the Tolerance Interval bounds around the predicted value 90 % of the time. The example has a relatively large sample size of 25, so the tolerance limits are only slightly wider than the 90 % single observation prediction limits. As the number of exposure conditions

increase, the Tolerance Interval approaches the Prediction Interval. The tolerance limits might be much wider when the sample size is small, therefore sample size should be chosen carefully relative to the desired uncertainty of the model. Note there are 3 observed data points that are outside the tolerance limits in Figure 3. This is not surprising as there remains a finite probability that points will fall outside the tolerance limits. If x samples in the population are not within the desired coverage probability D, then x follows a discrete binomial probability distribution with N trials and success probability of 1–D. The probability of x or more samples outside the Tolerance Interval is equal to 1 minus the probability of (x–1) or fewer samples outside the interval. Accordingly, the probability for 3 or more outliers from the 90 % Tolerance Interval within the 25 samples shown in Figure 3 is 46 %.

Therefore, the AIMD model prediction uncertainty has a distribution derived from the residual errors of a regression analysis which can be used directly as an input to a Monte Carlo type of error analysis. An estimate of u_{Predict} from the distribution can be made using a Tolerance Interval with specified population coverage and confidence level. In this case, the model output is within the range $[P_{\text{model}} \pm u_{\text{Predict}}]$ where $u_{\text{Predict}} = k^*\sigma$.

6.3 AIMD model uncertainty (u_{Predict}): Method 2

Method 2 can be used to determine the uncertainty in the measurement of the AIMD model that then propagates to the uncertainty (u_{Predict}) of the estimated power deposition of an AIMD hotspot.

Uncertainty budgets associated with the Piecewise Excitation method should account for process variation, sources of perturbation, measurement instrumentation uncertainty and sources of bias. The dominant sources of uncertainty of the piecewise excitation method are listed in Table 2. Sources of uncertainty with non-gaussian distributions should be converted to Gaussian using appropriate divisors. The combined standard uncertainty should be computed as the root sum square of the individual contributors. Guidance for distribution conversion and combination of various standard uncertainties is available in 4.3 and 5 of Reference [1], and in Reference [6].

Table 2 lists of dominant sources of uncertainty of the piecewise excitation technique for AIMD model generation. The sources of uncertainty corresponding to the appropriate model generation step are listed.

Table 2 — Dominant sources of uncertainty

Step		Source of uncertainty	Tolerance	Probability distribution	Divisor	Standard uncertainty
1	S_{hotspot} (z)	$E_{\tan}$ transmit antenna				
2	S_{hotspot} (z)	E-field scatter sense antenna				
3	S_{hotspot} (z)	Test and measurement instrumentation				
4	A	Measurement and power conversion uncertainty				
Combined standard uncertainty (RSS)						

Each source of uncertainty listed in Table 2 is described in greater detail below.

a) Sources of model generation uncertainty due to the transmit antenna might be attributed to:

   1) Positioning tolerance: The piecewise excitation method relies on the application of constant amplitude, constant phase piecewise excitation along the AIMD. Antennas exhibit steep gradients, especially in the reactive and radiative near fields. Therefore, variability in the spatial positioning of the excitation antenna in relation to the DUT is potentially a significant source of amplitude uncertainty. The positioning variability might take the form of misalignments caused by fixture tolerances or positioner tolerances. Care must be taken to correct for gross